Third-Order Elastic Moduli of Calcium Fluoride*

S. Alterovitz and D. Gerlich

Physics Department, Tel Aviv University, Ramat Aviv, Israel

(Received 17 December 1968)

The complete set of the room-temperature third-order elastic moduli of CaF_2 were determined from the change in the sound velocity under uniaxial compression. The measured values in units of 10^{11} dyn/cm^2 are $C_{111} = -124.6$, $C_{112} = -40.0$, $C_{123} = -25.4$, $C_{144} = -12.4$, $C_{166} = -21.4$, and $C_{456} = -7.5$. The experimentally measured third-order elastic moduli are compared with the theoretically calculated ones, and a good agreement is found. Conclusions pertaining to the lattice-force interactions are presented.

INTRODUCTION

A N appreciable number of studies of the third-order elastic moduli (TOEM) have been published over the past few years, owing to the enhanced interest in the anharmonic properties of solids.[1] Measurements of the complete set of the TOEM have been reported for materials in the alkali-halide system, the diamond structure semiconductors, several metals, and for barium fluoride. The alkaline-earth fluorides constitute a simple system of ionic crystals where every ion is not a center of inversion, thus raising the possibility of relative motion of the sublattices under stress. In addition, the experimentally measured TOEM of BaF_2 agree well with a theoretical calculation based on a simple central-force model.[2] There seems, therefore, to be an interest in extending the measurements of the TOEM to other members of the alkaline-earth fluoride group.

The present work reports measurements of the complete set of the TOEM of CaF_2 at room temperature. The experimental data were compared with the results of a theoretical calculation of the TOEM, and from this comparison some conclusions concerning the lattice-force model applicable to CaF_2 are drawn.

EXPERIMENTAL

The samples used for the present work were single crystals of CaF_2 purchased from the Harshaw Chemical Co. The crystals were cube shaped, size $15 \times 16 \times 17$ mm approximately, their faces corresponding to (110), ($1\bar{1}0$), and (001) crystalline planes. The crystals were hand lapped until the faces were parallel to within a few parts in 10^5. The orientation of the faces was then checked by x-ray Laue back-reflection, and was found to correspond to the crystalline planes to within $1°$.

Calcium fluoride, being cubic, has six independent TOEM, C_{111}, C_{112}, C_{144}, C_{166}, C_{123}, and C_{456}, the Thurston-Brugger[3] definitions of the TOEM being

used throughout. These moduli were determined from the variation of the sound velocity under uniaxial compression. With the available samples, nine different combinations of sound propagation modes and stresses could be utilized,[3] viz., the six different propagation modes under stress in the [$1\bar{1}0$] direction and the three different modes under stress in the [001] direction. Thus nine equations for the six TOEM are obtained, and the latter are computed by a least-squares fit. The sound waves were generated by means of X- and Y-cut crystalline quartz transducers, operating at their fundamental frequency of 15 Mc/sec. The transducers were bonded to the samples with phenylsalycilate (salol).

In order to prevent the cracking of the samples and to eliminate dislocation-line movement, which might falsify completely the results of the measurements,[4–6] the stress level was kept very low, never exceeding 30 kg/cm^2. In addition, the samples were irradiated with a γ-ray dose of 5000 R prior to the measurement. Such an irradiation creates additional pinning centers for the dislocation lines, thus preventing their motion.[6,7]

The changes in the sound velocity were determined by the McSkimin frequency-modulated pulse-superposition method,[8–10] using a shock-excited oscillator. Here the change in the sound velocity is proportional to the change in the reciprocal repetition rate resonant frequency[8]; thus, by determining the resonant frequency as a function of the applied stress, the change in sound velocity with stress may be determined. The temperature of the sample being investigated was monitored carefully during the entire time, and all the measurements were normalized to a temperature of $295°K$.

The stress was generated by means of a manually operated laboratory press, and measured with a factory-calibrated load cell. Lead shims were placed between the sample and the pressurizing surfaces in

* Based on a thesis submitted by S. Alterovitz to the Tel Aviv University in partial fulfillment of the requirements for the Ph.D. degree.

[1] G. Leibfried and W. Ludwig, in *Solid State Physics*, edited by F. Seitz and D. Turnbull (Academic Press Inc., New York, 1961), Vol. 12.

[2] D. Gerlich, Phys. Rev. **168**, 947 (1968).

[3] R. N. Thurston and K. Brugger, Phys. Rev. **133**, A1604 (1964).

[4] Y. Hiki and A. V. Granato, Phys. Rev. **144**, 411 (1966).

[5] K. Salama and G. A. Alers, Phys. Rev. **161**, 673 (1967).

[6] K. D. Swartz, J. Acoust. Soc. Am. **41**, 1083 (1967).

[7] R. Gordon and A. S. Nowick, Acta Met. **4**, 514 (1956).

[8] H. J. McSkimin, J. Acoust. Soc. Am. **33**, 12 (1964).

[9] H. J. McSkimin and P. Andreatch, Jr., J. Acoust. Soc. Am. **34**, 609 (1962).

[10] H. J. McSkimin and P. Andreatch, Jr., J. Acoust. Soc. Am. **41**, 1052 (1967).

order to prevent the application of shear stresses to the sample.

RESULTS

In Figs. 1 and 2, the measured reciprocal resonant frequencies for the different propagation modes as a function of the applied stress are shown. As can be seen, the changes in the sound velocity are linear up to the highest applied stress, which is a necessary condition for no dislocation-line movement to have occurred. The lines are least-squares fits to the experimental data.
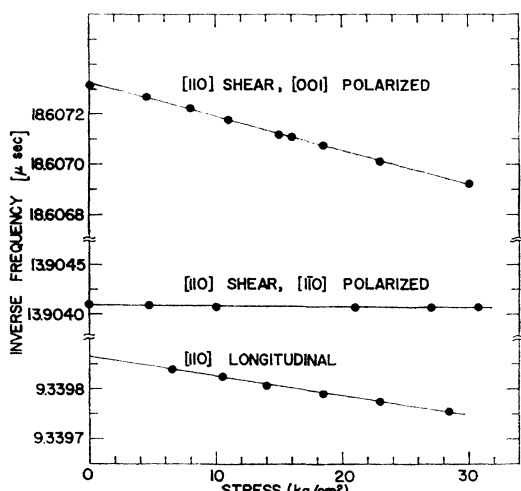

FIG. 1. Change in reciprocal resonant frequency versus uniaxial compression in the [001] direction for different propagation modes.
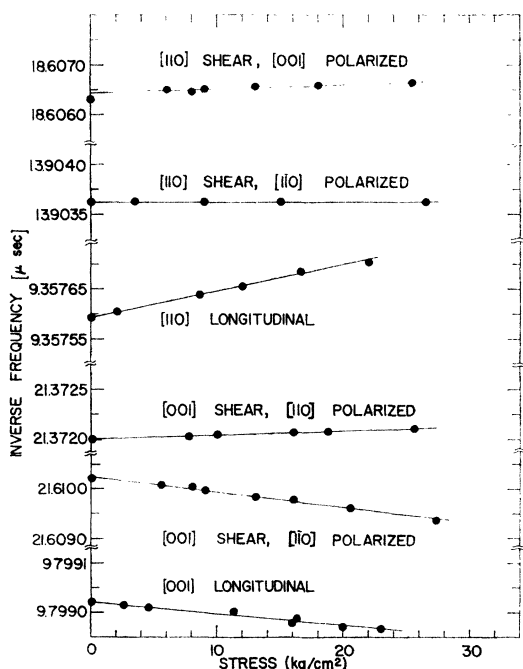

FIG. 2. Change in reciprocal resonant frequency versus uniaxial compression in the [1$\bar{1}$0] direction for different propagation modes.

From the slopes of these lines, the pressure derivatives at zero pressure of $\rho_0 W^2$, viz., $(\rho_0 W^2)_{P=0}'$, are determined. Here ρ_0 is the zero-pressure density and W is the natural velocity, defined as $2L_0/t$, where L_0 is the zero-pressure length of the sound path and t is the round-trip sound travel time. The values of $(\rho_0 W^2)_{P=0}'$ for the different propagation modes determined from the lines in Figs. 1 and 2 with their associated errors are shown in Table I. Also shown in the table are the average values of the various $(\rho_0 W^2)_{P=0}'$, designated as $\langle(\rho_0 W^2)_{P=0}'\rangle_{\text{av}}$, determined as the arithmetic average from a number of runs carried out for each propagation mode. As can be seen, the agreement between the typical and average $(\rho_0 W^2)_{P=0}'$ is within the limits of error in all cases except for mode 8. This is not surprising, because the latter mode is a somewhat "pathological" case.[11] From the values of $\langle(\rho_0 W^2)_{P=0}'\rangle_{\text{av}}$ in Table I, the six TOEM are computed, and are shown in Table II. The parameters required for the latter computation are presented in Table III.[12–15] Here the $c_{IJ}{}^S$ are the adiabatic second-order elastic moduli (SOEM). In

TABLE I. Typical and average values of $(\rho_0 W^2)_{P=0}'$ for the various propagation modes.

No. of mode	Propaga-tion direction	Displace-ment direction	Stress direction	$(\rho_0 W^2)_{P=0}'$	$\langle(\rho_0 W^2)_{P=0}'\rangle_{\text{av}}$
1	[110]	[110]	[001]	1.269±0.045	1.269
2	[110]	[1$\bar{1}$0]	[001]	0.186±0.012	0.192
3	[110]	[001]	[001]	0.529±0.006	0.526
4	[001]	[001]	[1$\bar{1}$0]	0.833±0.051	0.833
5	[001]	[1$\bar{1}$0]	[1$\bar{1}$0]	0.919±0.018	0.919
6	[001]	[110]	[1$\bar{1}$0]	−0.239±0.014	−0.219
7	[110]	[110]	[1$\bar{1}$0]	−1.248±0.090	−1.180
8	[110]	[1$\bar{1}$0]	[1$\bar{1}$0]	−0.039±0.0037	−0.0985
9	[110]	[001]	[1$\bar{1}$0]	−0.517±0.061	−0.469

order to normalize all measurements to 295°K, the temperature derivatives of the SOEM had to be evaluated. These derivatives were determined from the temperature variation of t in the five different available propagation modes over the temperature range 273–300°K. In this range the changes were found to be linear; the results are shown in Table IV. Here v is the sound velocity and T is the absolute temperature. From the data of Table IV, the temperature derivatives of the SOEM are computed by a weighted least-squares fit, the weights being the reciprocals of the standard deviations. The temperature derivatives together with similar data measured by Wong and Schuele[15] and by Haussühl[16] are presented in Table V. As can be seen, the

[11] H. J. McSkimin and P. Andreatch, Jr., J. Appl. Phys. 35, 3312 (1964).
[12] D. N. Batchelder and R. O. Simmons, J. Chem. Phys. 41, 2324 (1964).
[13] S. S. Todd, J. Am. Chem. Soc. 71, 4115 (1949).
[14] C. Wong and D. E. Schuele, J. Phys. Chem. Solids 28, 1225 (1968).
[15] C. Wong and D. E. Schuele, J. Phys. Chem. Solids 29, 1309 (1968).
[16] S. Haussühl, Phys. Status Solidi 3, 1072 (1963).

TABLE II. TOEM of CaF$_2$ (units are 10^{11} dyn/cm^2).

C_{111}	C_{112}	C_{123}	C_{144}	C_{166}	C_{456}
-124.6 ± 9.1	-40.0 ± 3.0	-25.4 ± 2.9	-12.4 ± 1.5	-21.4 ± 0.9	-7.48 ± 0.38

agreement between the present results and Haussühl's data is very good.

In order to ascertain that no dislocation-line movement has taken place during the uniaxial compression, the three linear combinations of the TOEM which are determined by hydrostatic pressure measurements, viz., $C_{111}+2C_{112}$, $C_{144}+2C_{166}$, and $2C_{112}+C_{123}$, as derived from the present data, were compared with the values obtained from hydrostatic pressure data.[14,15,17] This comparison is shown in Table VI, and, as can be seen, the agreement between the two sets indicates that probably no dislocation-line motion has occurred.

The errors indicated for the $(\rho_0W^2)_{P=0}'$ and the TOEM are the standard deviations obtained in the least-squares fit, multiplied by 0.675. This was found to provide the largest error. Several other error-evaluation procedures were attempted, and all gave smaller errors than the ones shown in Table II. First the method presented in Ref. 2 was tried, and the resulting errors for the TOEM were about half those shown in Table II. Then the errors due to temperature drift, the variation from crystalline direction of the setting of the shear transducers, and the frequency measurement were estimated and propagated through the entire calculation for the TOEM. The resulting errors in the latter quantities were still smaller than those indicated in Table II.

TABLE III. Data required for the computation of the TOEM of CaF$_2$. (Temperature is 295°K.)

Density[a]	3.1799 g/cm^3
Coefficient of linear thermal expansion[b]	1.88×10^{-5} deg^{-1}
Specific heat at constant pressure[c]	66.89 J mole^{-1} deg^{-1}
$c_{11}{}^{S}$ [d,e]	16.42×10^{11} dyn/cm^2
$c_{12}{}^{S}$ [d,e]	4.398×10^{11} dyn/cm
$c_{44}{}^{S}$ [d,e]	3.370×10^{11} dyn/cm$_2$

[a] Measured experimentally.
[b] Reference 12.
[c] Reference 13.
[d] Reference 14.
[e] Reference 15.

TABLE IV. Temperature dependence of the sound travel time.

No. of mode	Propagation direction	Displacement direction	ρv^2	dt/dT (psec/deg)
I	[110]	[110]	$\frac{1}{2}(c_{11}+c_{12}+2c_{44})$	1046.1 ± 9.2
II	[001]	[001]	c_{11}	938.7 ± 5.6
III	[110]	[1$\bar{1}$0]	$\frac{1}{2}(c_{11}-c_{12})$	1079.5 ± 1.8
IV	[110]	[001]	c_{44}	3047.8 ± 10.4
V	[001]	(1$\bar{1}$0) plane	c_{44}	3481.6 ± 2.0

[17] P. S. Ho and A. L. Ruoff, Phys. Rev. **161**, 864 (1967).

DISCUSSION

In the following discussion, lower-case letters will denote tensorial indices, while capital letters will denote the Voigt notation. The TOEM measured in the present work are mixed TOEM, being the isothermal pressure derivatives of the adiabatic SOEM.

$$C_{jrksip}= (\partial c_{jrks}{}^{S}/\partial\eta_{ip})_{T,P=0}, \tag{1}$$

where η_{ip} are the Lagrangian strains. In theoretical calculations, the adiabatic TOEM are usually calculated,[18,19] the latter being defined as

$$C_{jrksip}{}^{S}= (\partial c_{jrks}{}^{S}/\partial\eta_{ip})_{S,P=0}. \tag{2}$$

The difference between these two types of TOEM is given by[20]

$$\delta_{JRK}=C_{JRK}{}^{S}-C_{JRK}=\frac{T\alpha}{\rho_0 C_P}(\sum_{M=1}^{3} c_{KM}{}^{S})$$

$$\times\left[\alpha\sum_{L=1}^{3}C_{JRL}-\left(\frac{\partial c_{JR}{}^{S}}{\partial T}\right)_P\right]. \tag{3}$$

Here α is the linear thermal expansion coefficient and C_P is the specific heat at constant pressure. The relative differences δ_{JRK}/C_{JRK} are shown in Table VII. As can be seen, the δ_{JRK} are negligible with respect to the

TABLE V. Temperature dependence of the SOEM of CaF$_2$. (Units are 10^{-4} deg^{-1}.)

	$(\partial \ln c_{11}/\partial T)_P$	$(\partial \ln c_{12}/\partial T)_P$	$(\partial \ln c_{44}/\partial T)_P$
Haussühl[a]	-2.05	-2.91	-3.43
Wong and Schuele[b]	-1.94	-2.39	-3.62
Present data	-2.05	-2.82	-3.40

[a] Reference 16.
[b] Reference 15.

TABLE VI. Values of $C_{111}+2C_{112}$, $C_{144}+2C_{166}$, and $2C_{112}+C_{123}$ as derived separately from uniaxial and hydrostatic pressure measurements. (Units are 10^{11} dyn/cm^2.)

Method of stress	$C_{111}+2C_{112}$	$C_{144}+2C_{166}$	$2C_{112}+C_{123}$
Uniaxial	-204.6	-55.2	-105.4
Hydrostatic[a]	-189.1	-59.8	-86.6
Hydrostatic[b]	-189.4	-60.0	-86.5
Hydrostatic[c]	-204.7	-61.0	-129.9

[a] Reference 14.
[b] Reference 15.
[c] Reference 17.

[18] P. B. Ghate, Phys. Rev. **139**, A1666 (1965).
[19] R. Srinivasan, Phys. Rev. **165**, 1054 (1968).
[20] K. Brugger, Phys. Rev. **133**, A1611 (1964).

TABLE VII. Relative difference between the adiabatic
and mixed TOEM (in %).

111	112	123	144	166	456
0.2	0.6	1.5	0	0	0

experimental errors, and for comparison with theory, the mixed TOEM may be safely used.

Generally, the SOEM depend on volume and temperature. The measured temperature dependence of the SOEM will be given as a sum of an explicit and implicit temperature dependence, the latter being caused by the change of volume with temperature[21]:

$$\left(\frac{\partial \ln c_{JR}{}^S}{\partial T}\right)_P = \left(\frac{\partial \ln c_{JR}{}^S}{\partial T}\right)_V + \frac{\alpha}{c_{JR}{}^S} \sum_{Q=1}^{3} C_{JRQ}. \qquad (4)$$

Here the first term on the right is the explicit temperature dependence, while the second term is the volume-dependent part. Utilizing the measured TOEM and temperature dependence of the SOEM, the explicit temperature-dependent part may be evaluated. The three terms shown in Eq. (4) are shown in Table VIII for the three SOEM of CaF₂. The discrepancy between the values in the latter table and those of Table VI of Wong and Schuele[14] seems to be due to the fact that the latter authors have used the pressure derivatives $[\partial(\rho v^2)/\partial P]_{P=0}$ which are not equal to the corresponding thermodynamic pressure derivatives $(\partial c_{JR}{}^S/\partial P)_{P=0}$,[20] the latter being the ones which are used in Eq. (4). As

TABLE VIII. Values of the measured, explicit, and implicit temperature dependence of the SOEM of CaF₂ at room temperature. (Units are 10⁻⁴ deg⁻¹.)

	$\left(\dfrac{\partial \ln c_{JR}{}^S}{\partial T}\right)_P$	$\left(\dfrac{\partial \ln c_{JR}{}^S}{\partial T}\right)_V$	$\dfrac{\alpha}{c_{JR}{}^S} \sum\limits_{Q=1}^{3} C_{JRQ}$
$c_{11}{}^S$	−2.05	0.19	−2.34
$c_{12}{}^S$	−2.82	1.67	−4.49
$c_{44}{}^S$	−3.40	−0.33	−3.07

[21] D. Lazarus, Phys. Rev. **76**, 545 (1949).

can be seen from Table VIII, the temperature dependence of c_{44} for CaF₂ is almost entirely due to the volume change.

Assuming a model of central-force interactions, consisting of Coulomb forces and overlap forces between nearest and next-nearest neighbors, the TOEM have been evaluated theoretically for the fluorite structure.[18] The calculation has been carried out for a rigid-ion and a shell model. A comparison between the experimental results and the theoretical calculation is shown in Table IX. It is obvious that the agreement between experiment and theory is very good, especially bearing in mind the fact that we are concerned with quantities which are measured by a second-order effect. Note also that the theoretical calculation of the TOEM is for 0°K, while our measurements are at 295°K, but the change between 0 and 295°K is not expected to be more than

TABLE IX. Comparison of experimental and theoretical TOEM of CaF₂. (Units are 10¹¹ dyn/cm².)

	C_{111}	C_{112}	C_{123}	C_{144}	C_{166}	C_{456}
Expt.	−124.6	−40.0	−25.4	−12.4	−21.4	−7.5
Theor.—rigid-ion model	−95.5	−44.2	−27.9	−17.0	−29.4	−8.8
Theor.—shell model	−95.5	−44.2	−27.9	−11.4	−25.3	−9

20–30%.[16] It is also interesting to note that the largest discrepancy between the experimental data and theoretical results occurs for C_{111}, which is also the case for barium fluoride.[2] This agreement between experiment and theory indicates that the simple model of central-force interaction is apparently a satisfactory description of the lattice forces in the case of CaF₂, a conclusion similar to that obtained for BaF₂. Hence, the violation of the Cauchy relations for the TOEM of CaF₂ must be caused by internal relative displacements of the two sublattices, and is probably not due to many-body forces.

ACKNOWLEDGMENT